Chemical Engineering Science 142 (2016) 79–88

Contents lists available at ScienceDirect

Chemical Engineering Science

journal homepage: www.elsevier.com/locate/ces

A probabilistic approach to radiant field modeling in dense particulate systems

A. Busciglio [a,*], O.M. Alfano [c], F. Scargiali [b], A. Brucato [b]

[a] Dipartimento di Chimica Industriale 'Toso Montanari', Alma Mater - Universitá di Bologna, Via Terracini 28 - 40131 Bologna BO - Italy
[b] Dipartimento di Ingegneria Chimica, Gestionale, Informatica e Meccanica, Universitá degli Studi di Palermo, Viale delle Scienze, Ed. 6 - 90128 Palermo - Italy
[c] INTEC, Instituto de Desarrollo Tecnologico para la Industria Quimica, Universidad Nacional del Litoral and CONICET, Guemes 3450, (3000) Santa Fe, Argentina

HIGHLIGHTS

- Radiant fields in dense, size–distributed, particulate suspensions were modeled.
- A probabilistic approach for computing the characteristic photon extinction length was developed.
- Monte Carlo simulations were used to validate the model.
- The proposed model correctly predicts radiation fields up to 30%v/v of particles.

ARTICLE INFO

Article history:
Received 14 May 2015
Received in revised form
3 November 2015
Accepted 25 November 2015
Available online 5 December 2015

Keywords:
Photo-catalysis
Photo-bioreactors
Radiant field modeling
Dense particulate system
Monte Carlo simulation

ABSTRACT

Radiant field distribution is an important modeling issue in many systems of practical interest, such as photo-bioreactors for algae growth and heterogeneous photo-catalytic reactors for water detoxification.

In this work, a simple radiant field model suitable for dispersed systems showing particle size distributions, is proposed for both dilute and dense two-phase systems. Its main features are: (i) only physical, independently assessable parameters are involved and (ii) its simplicity allows a closed form solution, which makes it suitable for inclusion in a complete photo-reactor model, where also kinetic and fluid dynamic sub-models play a role. A similar model can be derived by making use of concepts developed in the realm of stereology. The resulting equation is similar, yet not identical, to that obtained with the probabilistic approach, due to the fact that in stereology the front plane, or the focus plane, may well cut through particles, a circumstance excluded both in the probabilistic model and in actual photoreactors.

The two models are compared with pseudo-experimental data obtained by means of Monte Carlo simulations, and the probabilistic model is found to give rise to the best agreement.

1. Introduction

As far as radiation transfer is concerned, particle-fluid dispersions belong to the class of scattering-absorbing media. The need to model radiation intensity distribution in such media occurs in a number of important applications, including autotrophic microalgae growth (Molina Grima et al., 1999; Yun and Park, 2001; Li et al., 2003; Heinrich et al., 2013), hydrogen production by photosynthetic bacteria (Katsuda et al., 2000), as well as heterogeneous photo-catalytic reactors for water and air purification (Cassano and Alfano, 2000; Li Puma et al., 2004; Brucato et al., 2006; Otalvaro-Marin et al., 2014), hence processes aimed at addressing significant energetic and environmental problems.

Clearly reliable tools for the design and development of photo-bioreactors and heterogeneous photo-catalytic reactors are required in order to successfully bring these processes to the industrial stage. Mathematical modeling of the radiant field in photoreactors has been the subject of a number of studies (Katsuda et al., 2000; Li et al., 2003; Su et al., 2003; Brucato et al., 2006; Palma et al., 2010; Motegh et al., 2013). The ability to model the radiant field in a photo-reactor is of paramount importance also to obtain reliable intrinsic kinetic data from experiments (Davydov et al., 1999).

* Corresponding author.
E-mail addresses: antonio.busciglio@unibo.it (A. Busciglio), alfano@intec.unl.edu.ar (O.M. Alfano), francesca.scargiali@unipa.it (F. Scargiali), alberto.brucato@unipa.it (A. Brucato).

http://dx.doi.org/10.1016/j.ces.2015.11.025
0009-2509/

In general, when chemical effects are involved, radiation field modeling is a very complex task, especially because the reactants' concentration field may strongly influence the radiation field (Brucato and Rizzuti, 1997a). However, in heterogeneous photo-catalytic reactors as well as in algae photo-bioreactors, discrete particles absorb and scatter light independently of reactants or substrates that are often transparent to the radiation wavelengths involved in the activation of photo-catalyst (or chloroplasts). In these cases, the radiation field, being independent from the particle concentration field, can be computed in advance.

Moreover, the interactions between the radiant source and the dispersed particles, that can both scatter and absorb photons, make radiant field modeling a very complicated task. A solution of the Radiation Transfer Equation (RTE) would be required, but analytical solutions are possible only in very simple cases (Cassano et al., 1995; Cassano and Alfano, 2000; Brucato et al., 2006).

Hence, the following alternative approaches have been proposed to obtain approximate solutions of the RTE: (i) numerical solution based either on discrete ordinate method (Santarelli, 1985; Brandi et al., 1996; Romero et al., 1997; Brandi et al., 1999, 2000) or Monte Carlo method (Spadoni et al., 1978; Pasquali et al., 1996; Heinrich et al., 2012); (ii) analytical solution of simplified radiant field models (Brucato et al., 2006; Brucato and Rizzuti, 1997a, 1997b; Li Puma and Brucato, 2007) which, though approximate, give a quick physical idea of the process key parameters, which is what is really useful for equipment design and optimization.

In all of the aforementioned models, only dilute particle suspensions were considered. The case of highly concentrated single-sized particle suspensions was afforded by means of a probabilistic approach in a previous publication (Brucato et al., 1997). In the present work, the same approach is further developed by extending it to the case of concentrated suspensions of particles with size distributions. The resulting model is validated by comparison with pseudo-experimental data obtained via a Monte Carlo approach as well as with similar equations obtained in the realm of stereology (Overby and Johnson, 2005).

2. Probabilistic model

In previous investigations (Brucato and Rizzuti, 1997a, 1997b; Brucato et al., 2006), a modeling approach based on particle shielding considerations led to a simplified (closed form) model which was also experimentally validated. The present model is practically based on the same set of assumptions, apart for the assumption of single sized particles, which is removed. Hence the basic assumptions of the model are the following:

- plane (slab) photo-reactor;
- particles are large enough in order for geometric optics to hold true;
- particles are randomly dispersed;
- an homogeneous, transparent fluid is considered (it does no absorb or scatter any radiation);
- there is no emission by the heterogeneous system;
- uniform, orthogonal irradiation of the front wall of the reactor is considered;
- photons can only move in a uni-directional forward direction;
- any particle cross sectional area $a_{p,i}$ is much smaller than photoreactor front wall area, so that the condition $a_{p,i} \ll A$ is always true.

It is worth reminding that the so-called Zero Reflectance Model (ZRM) was validated by means of experimental data (Brucato and Rizzuti, 1997a): so the assumptions here adopted, especially those regarding the optical properties of both fluid and particles can be considered valid. Clearly, in industrial systems, as well as in more complex system geometries, the photon absorption and scattering due to the fluid, back- and lateral- scattering phenomena (and so on) have to be considered (Brucato et al., 2006), but their effect is out of the scope of the present investigation.

Let us first consider the case in which any photon-particle interaction results in photon absorption by the particle itself, *i.e.* a case akin to the ZRM introduced by Brucato and Rizzuti (1997a).

A control volume having size $V = AL$ is considered, where the A surface coincides with the reactor front wall and L is reactor thickness. For each of the N_p particles within the control volume, let us now consider the generic π_i plane (parallel to the reactor wall) intercepting the relevant i-th particle at its maximum cross section, as shown in Fig. 1. At any given instant, all these planes can be numbered starting from the front wall of the reactor towards the rear wall. Therefore, plane π_1 is the plane pertaining to the first closest particle to reactor wall, plane π_2 to the second closest particle and so on, up to the π_{N_p}-th plane, pertaining to the particle closest to the rear reactor wall.

Let us now consider a photon entering from the front wall. Under the following assumption:

- Each particle-photon interaction always results into photon absorption (*Zero Reflectance Model* assumption).

The probability P_1 for the photon to survive to the first plane can be expressed as:

$$P_1 = \left(1 - \frac{a_{p,1}}{A}\right) \tag{1}$$

where $a_{p,1}$ is the cross sectional area of the first particle.

2.1. Dilute dispersions

If the suspension is sufficiently dilute, the second plane is sufficiently spaced from the first in order for the relevant particle be able to freely occupy all positions in the plane. The probability P_2 can be computed exactly as for P_1:

$$P_2 = \left(1 - \frac{a_{p,2}}{A}\right) \tag{2}$$

Hence, the following assumption is added to the assumptions set:

- A suspension can be considered dilute when each particle can freely occupy the whole relevant plane π_i without being affected by the presence of particles in previous planes π_{i-1}, π_{i-2}, etc., or subsequent planes π_{i+1}, π_{i+2}, etc.

In case of dilute suspensions, Eq. (2) holds true for all particles and the probability that the photon would have to survive all the N_p planes is simply given by the product of the probabilities the photon has to survive each plane. Notably, this compound probability coincides with the probability that the photon exits the photoreactor from the rear wall, *i.e.* with the fraction of photons reaching the distance L:

$$\frac{G}{G_0} = \prod_{i=1}^{N_p} P_i = \prod_{i=1}^{N_p} \left(1 - \frac{a_{p,i}}{A}\right) \tag{3}$$

By taking the logarithm of both sides of Eq. (3), and remembering that $\ln(1+x) \approx x$ for $0 < x \ll 1$:

$$\ln \frac{G}{G_0} = \sum^{N_p} \ln \left(1 - \frac{a_{p,i}}{A}\right) \approx -\sum^{N_p} \frac{a_{p,i}}{A} = -\frac{1}{A} \sum^{N_p} a_{p,i} \tag{4}$$

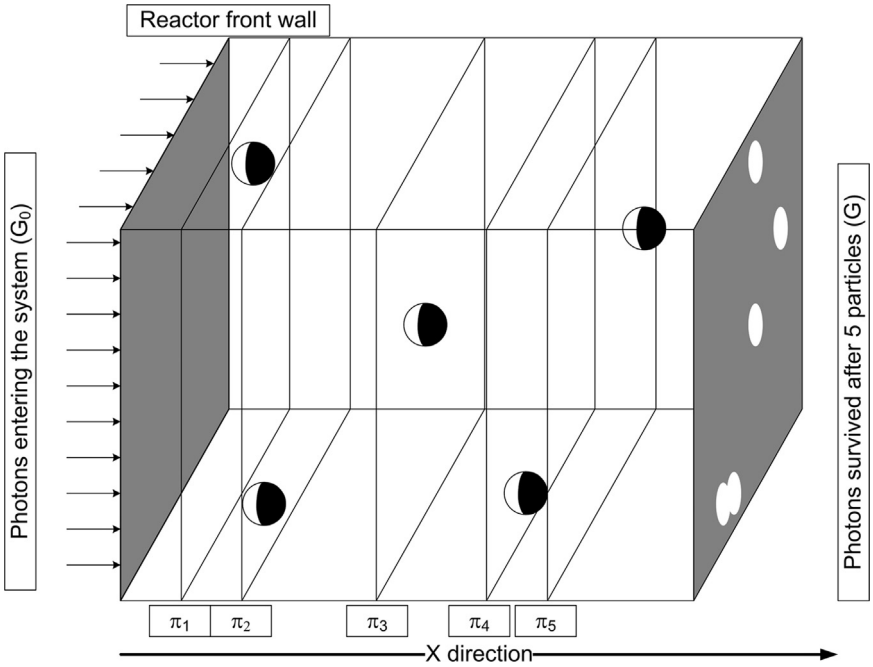

Fig. 1. System scheme in case of dilute suspension.

Some manipulation is needed in order to write Eq. (4) in a form in which only assessable parameters appear. At first, one may write the overall particle volume contained within the control volume as a function of particle volume fraction, or as the sum of individual particle volumes:

$$\phi AL = \sum^{N_p}\left(\alpha d_{p,i}^3\right) = \alpha\sum^{N_p} d_{p,i}^3 \tag{5}$$

where ϕ is the particle volume fraction and α is the proportionality factor between particle volume and particle size cubed, here assumed as a constant for all particles, regardless of their size. Clearly, the value of the α factor depends on particle shape. Also, the sum of projected areas can be written as:

$$\sum^{N_p} a_{p,i} = \sum^{N_p} \beta d_{p,i}^2 = \beta\sum^{N_p} d_{p,i}^2 \tag{6}$$

By substituting into Eq. (4) both Eq. (6) and the A term as obtained from Eq. (5), the following equality is obtained:

$$\ln\frac{G}{G_0} = -\frac{\beta\sum d_{p,i}^2\phi L}{\alpha\sum d_{p,i}^3} = -\frac{L}{\lambda_0} \tag{7}$$

where

$$\lambda_0 = (\alpha/\beta)\frac{d_{32}}{\phi} \tag{8}$$

which practically coincides with the similar equation obtained, with a rather different modeling approach, by Brucato and Rizzuti (1997a) in the case of single-sized particles. The only difference being that the Sauter mean diameter d_{32} is employed in place the particle diameter for single sized particles. Notably, the experimental validation of the *Zero Reflectance Model* provided by Brucato and Rizzuti (1997a) may be regarded as a cross-validation of the present approach as well.

2.2. Dense dispersions

With the present probabilistic approach it is possible to remove the hypothesis of dilute suspension. The case of concentrated suspension differs from that of dilute suspension as it cannot be assumed anymore that the distance between two subsequent planes π_i and π_{i+1} is large enough for the $i+1$-th particle to occupy any of the positions on the π_{i+1} plane. This is apparent from Fig. 2. If the distance between two subsequent plane i-th and $(i+1)$-th is smaller the sum of i-th and $(i+1)$-th particle radii, hence some of the positions in the $(i+1)$-th plane cannot be occupied by the relevant particle because of the presence of the i-th particle (Brucato et al., 1997).

This steric inhibition affects the probability of photon interception. Let us consider two subsequent planes π_{i-1} and π_i, and assume that they are so close that they practically coincide. If a photon has already survived to the $(i-1)$-th plane, it cannot lie on the cross section of $(i-1)$-th particle, otherwise it would have not survived to that plane. Therefore it certainly crosses the i-th plane elsewhere. It is clear that for this photon the probability of surviving to i-th plane is given by:

$$P_i = \left(1 - \frac{a_{p_i}}{\psi_i A}\right) \tag{9}$$

where the ψ_i is the fractional area of plane π_i available for the i-th particle to be placed. Notably, if two planes almost coincident are considered, the area inhibited to the i-th particle is a circle having radius equal to the sum of particle diameters $(r_{i-1}+r_i)$. If the particles have the same size, such inhibited area is equal to $4a_{p,i-1}$. Hence, the available area for the i-th particles can be written as:

$$\psi_i = \frac{A - a_{p,i-1}}{A} = 1 - \frac{4a_{p,i-1}}{A} \tag{10}$$

If the two planes are close but not coincident, the steric inhibition is less pronounced, and the freedom of the i-th particle to occupy positions on its plane is greater than in the above case, so that only a fraction of $4a_{p,i-1}$ has to be subtracted from the whole area A, see Fig. 2 for a visual example. Hence, it seems reasonable to generalize Eqs. (9) and (10) introducing a factor χ whose values range from 0 (planes spacing larger than half the sum of particle diameters, so that no steric interaction may occur) to 4 (in case of planes almost coincident and equally sized particles). Notably, the upper limit also depends on the sizes of the particles, so it can not

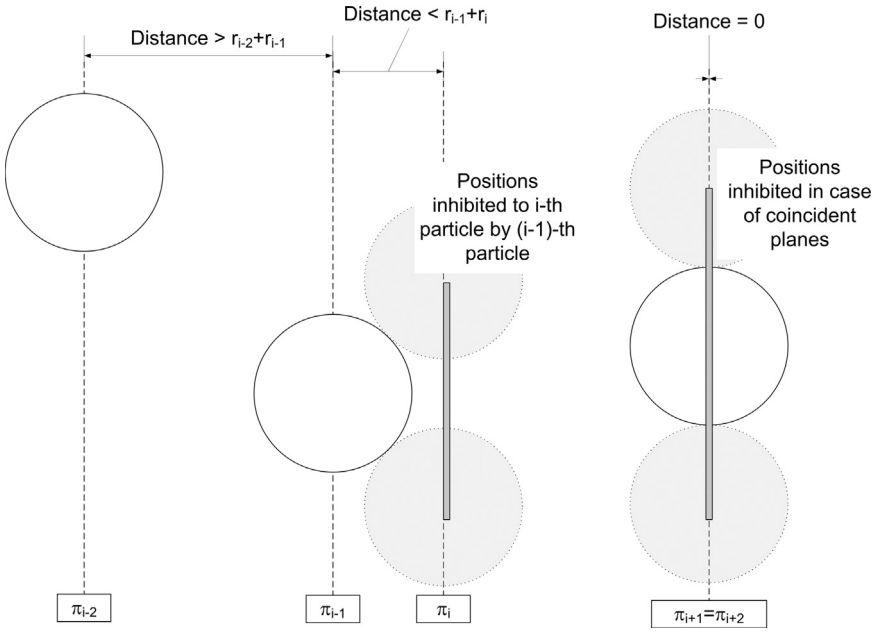

Fig. 2. Possible steric hindrance effects in case of concentrated suspensions.

be regarded as a general upper bounding limit.

$$\psi_i = \frac{A-\chi_{i-1}a_{p,i-1}}{A} = 1-\frac{1}{A}\left(\chi_{i-1}\beta d_{p,i-1}^2\right) \tag{11}$$

In addition, it is possible that more than one particle interacts with the placement of the i-th particle. Strictly speaking, all particles lying on planes closer to the front reactor wall should be considered. However, this can be simplified if one considers that the factor χ rapidly becomes nil when relevant plane has a distance larger than half the sum of the i-th and j-th particle diameters. Keeping in mind the meaning of the χ parameter, it is necessary to define an appropriate average value to be used in practical calculations. One may assume that the number N_i of particles to be considered as potentially giving steric inhibition to the placement of the i-th particle equals the number of particles statistically present in the volume comprised between plane π_i and a plane placed at a distance $d_{p,av}$ in front of it. Hence, a more general form of Eq. (11) may be written in order to account for the steric inhibition given by the above discussed N_i particles.

$$\psi_i = 1-\frac{\beta}{A}\sum_{j=1}^{N_i}\chi_{i-j}d_{p,i-j}^2 \tag{12}$$

where the N_i number of particles potentially producing steric inhibition effects on i-th particle are, on average, those contained within a control volume of area A and thickness $d_{p,av}$ along photon path. The volume of particles within the above defined volume can be expressed as a function of particle concentration, or as the sum of particle volumes, hence:

$$\phi A\, d_{p,av} = \sum_{j=1}^{N_i}\alpha d_{p,i-j}^3 \tag{13}$$

Eq. (13) may be rewritten as:

$$A = \frac{\alpha\sum_{j=1}^{N_i} d_{p,i-j}^3}{\phi\, d_{p,av}} \tag{14}$$

By defining an average value for the $\chi_{av,i}$ such that:

$$\sum_{j=1}^{N_i}\chi_{i-j}d_{p,i-j}^2 = \chi_{av,i}\sum_{j=1}^{N_i} d_{p,i-j}^2 \tag{15}$$

and substituting Eqs. (14) and (15) into Eq. (12), one obtains:

$$\psi_i = 1-\frac{\beta\phi d_{p,av}}{\alpha\sum_{j=1}^{N_i} d_{p,i-j}^3}\chi_{av,i}\sum_{j=1}^{N_i} d_{p,i-j}^2 = 1-d_{p,av}\chi_{av,i}\frac{\beta\phi}{\alpha d_{32}} = 1-\frac{\chi_{av,i}d_{p,av}}{\lambda_0} \tag{16}$$

The result shown in Eq. (16) may be used in combination with Eq. (9) to estimate the survival probability of a photon and therefore the extinction length λ_{Pr} obtained with the present probabilistic approach:

$$\ln\frac{G}{G_0} = \sum^{N_p}\ln\left(1-\frac{a_{p,i}}{\psi_i A}\right) \approx -\frac{1}{A}\sum^{N_p}\frac{a_{p,i}}{\psi_i} = -\frac{\beta}{A}\sum^{N_p}\frac{d_{p,i}^2}{1-\chi_{av,i}d_{p,av}/\lambda_0}$$
$$= -\frac{1}{1-\chi_{av,i}d_{p,av}/\lambda_0}\frac{\beta}{A}\sum^{N_p} d_{p,i}^2 \tag{17}$$

where the $\chi_{av,i}$ is the only parameter to be determined, while all other quantities are simple-to-determine properties of the suspension. The relevant average value χ_{av} can be in principle be derived from simulations, or in simple cases, it could be determined theoretically by means of geometric considerations. Again, Eq. (5) can be used to express A as a function of suspension properties, finally leading to the following equation formally identical to Lambert-Beer equation:

$$\ln\frac{G}{G_0} = -\frac{L}{\lambda_{Pr}} \tag{18}$$

where the corrected value of the extinction length λ is calculated as:

$$\lambda_{Pr} = \lambda_0\left(1-\frac{\chi_{av}d_{p,av}}{\lambda_0}\right) \tag{19}$$

For the case of dilute suspensions, $\phi \ll 1$ hence $\lambda_0 \gg d_{32}$ and $\lambda_0 \gg d_{p,av}$; in this case, considering that $\chi_{av} < 1$, Eq. (19) provides $\lambda \approx \lambda_0$ as expected. Notably, an increase of volume fraction decreases both factors in Eq. (19), giving rise to λ_{Pr} values progressively smaller than λ_0.

3. Stereological model

Similar results can be also obtained by using a completely different approach. When micrographs are taken in consideration,

i.e. 2D representations of 3D objects whose properties such as volumetric fraction and average size are of interest, *stereology* is the discipline that studies the methods to assess 3D properties from the available 2D data. In addition, when the image depth of field L is comparable or larger than the characteristic sizes of the objects of interest, the problem of accounting for the apparent objects overlap in 2D images of the system has to be considered.

One of the most important properties to unfold from 2D images is the volume fraction of objects ϕ within a control volume of size $A \times L$, knowing only the fractional image area occupied by the projected objects in a 2D image A'_A. Notably, this quantity is akin to the cross sectional area occupied by particles in a photoreactor, *i.e.*:

$$A'_A = 1 - \frac{G}{G_0} \tag{20}$$

In case of zero-thickness material slices ($L=0$), it can be shown that a simple relation exists between 2D and 3D properties (Delesse condition):

$$A'_A = \phi \tag{21}$$

However, this is not the case in many microscopy techniques, and has no practical relevance when applied to photoreactor application. When increasing the depth of field L, more objects enter within the image, increasing the apparent object density of the image. This phenomenon, also known as overprojection leads to a second confounding effect, since different individual objects may occupy the same location in the projected image, hence obscuring each other (Overby and Johnson, 2005).

The stereological approach to the depth of field problem is based on the formulation of a suitable differential equation to describe the change in projected area as a function of depth of field thickness. The only assumptions for this equation to be valid is that the structures under investigation are randomly distributed, and that in their respect, the plane is randomly placed and oriented. No assumption is made about the shape of the structure under investigation, or its volume fraction. The final result proposed by Overby and Johnson (2005), rewritten according to present paper concepts and nomenclature, is:

$$\begin{aligned} A'_A &= 1 - (1-\phi)\exp\left[-\frac{S_v L}{4(1-\phi)}\right] \\ \frac{G}{G_0} &= (1-\phi)\exp\left[-\frac{S_v L}{4(1-\phi)}\right] \\ \ln\frac{G}{G_0} &= \ln(1-\phi) - \frac{S_v L}{4(1-\phi)} \\ \ln\frac{G}{G_0} &= \ln(1-\phi) - \frac{L}{\lambda_{St}} \end{aligned} \tag{22}$$

where

$$\lambda_{St} = \frac{4(1-\phi)}{S_v} \tag{23}$$

Further details on the derivation of this equation were not reported here for the sake of brevity, but the interested reader can find the derivation in Overby and Johnson (2005). The extinction length λ_{St} is a function of particle volume fraction ϕ and specific interfacial area S_v (the interfacial area between the particles and the fluid per unit volume of the suspension), whose value can be inferred once the particle volume fraction and the relevant d_{32} are known. In the case of spherical particles, it is well known that:

$$S_v = \frac{6\phi}{d_{32}} \tag{24}$$

By substituting of Eq. (24) into Eq. (23), the following result is obtained

$$\lambda_{St} = (2/3)\frac{1-\phi}{\phi} d_{32} \tag{25}$$

Notably, different functional dependencies are found, both in the light extinction expression (compare Eqs. (18) and (22)) and in the extinction length (Eqs. (19) and (25)). For the sake of comparison, in the case of spherical particles ($\alpha = \pi/6$, $\beta = \pi/4$) the following extinction length expressions are obtained from the dilute, probabilistic (assuming $d_{p,av} \equiv d_{32}$) and stereological models respectively:

$$\lambda_0 = (2/3)\frac{d_{32}}{\phi} \tag{26}$$

$$\lambda_{Pr} = (2/3)\frac{d_{32}}{\phi}(1 - \chi_{av}\phi) \tag{27}$$

$$\lambda_{St} = (2/3)\frac{d_{32}}{\phi}(1-\phi) \tag{28}$$

4. Monte Carlo simulation

The Monte Carlo approach (Hammersley and Handscomb, 1983) was used to set up simulations aimed at the validation of the proposed model. Pseudo-experimental photon transmission data were obtained for systems having different particle concentrations and particle size distributions (*PSD*). The pseudo-experimental information on photon extinction so obtained can be compared with relevant values calculated by Eqs. (18) and (22).

Three different *PSDs* were investigated: single-sized particles, normally distributed particles and exponentially distributed particles. For comparison purposes, all distributions had the same d_{10}, but quite different shapes and Sauter diameters, as it can be appreciated in Fig. 3.

For each distribution, several particles concentration values were simulated, ranging from dilute suspensions ($\phi = 0.005$) to concentrated ones ($\phi = 0.30$). For each concentration, different reactor thicknesses were investigated ($L/d_{10} = 5-60$).

In practice, a realistic particle sample (larger than $N_p = 10^4$ particles) obeying a given distribution was preliminarily created by means of simple pseudo-random number generators. All particles were then placed within a control volume of fixed cross sectional area $A = l \times l$ and width L. The L value represents the width of the photo-reactor under investigation. For each value of the L depth and the ϕ values that has to be simulated, the A value

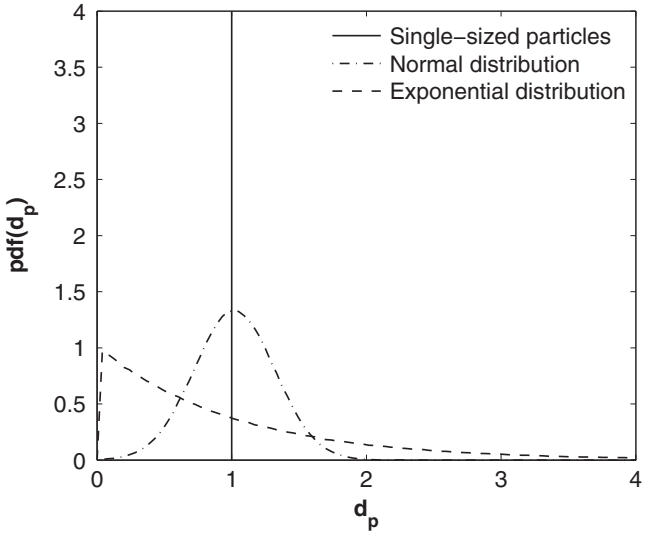

Fig. 3. *PSD* adopted for Monte Carlo simulations of photo-reactor. Single-sized particles: $d_{10} = 1$; Normal distribution: $d_{10} = 1$, $d_{32} = 1.164$; Exponential distribution: $d_{10} = 1$, $d_{32} = 2.98$.

must satisfy the following equality:

$$L \cdot A \cdot \phi = \sum_{N_p} V_{p,i} = \sum_{N_p} \frac{\pi d_{p,i}^3}{6} \tag{29}$$

In all cases, it is ensured that the relevant l values are large with respect to the mean particle size to make wall effects negligible. A suitable algorithm was then used to avoid particles overlap (Busciglio et al., 2010).

In Fig. 4, three examples of virtual boxes filled with normally distributed particles are shown for the cases of 1%, 10% and 25% particle volume fractions respectively.

For each virtual box created, an array of 62,500 photons were launched along the z direction. The central portion of the front box was used for the photon injection in order to avoid wall effect on the transmittance calculation. The ratio between the number of photons not intercepting any particle and the initial photon number was therefore computed, being equal to G/G_0. This simulation was repeated for at least 100 different virtual boxes for any given L value (that is a grand total of at least $6.25 \cdot 10^6$ photons launched for any simulation), in order to achieve statistical reliability.

5. Results

For each *PSD* analyzed, different particle volume fractions were analyzed, in order to assess the effect of particle concentration ϕ on radiant field. In Fig. 5, the simulated values of extinction ratio are reported as a function of traveled distance L in the case of normally distributed particles ($d_{10} = 1$, $d_{32} = 1.164$). Results obtained in simulations ran with different particle concentration values (ranging from $\phi = 0.005$ to $\phi = 0.30$) are reported.

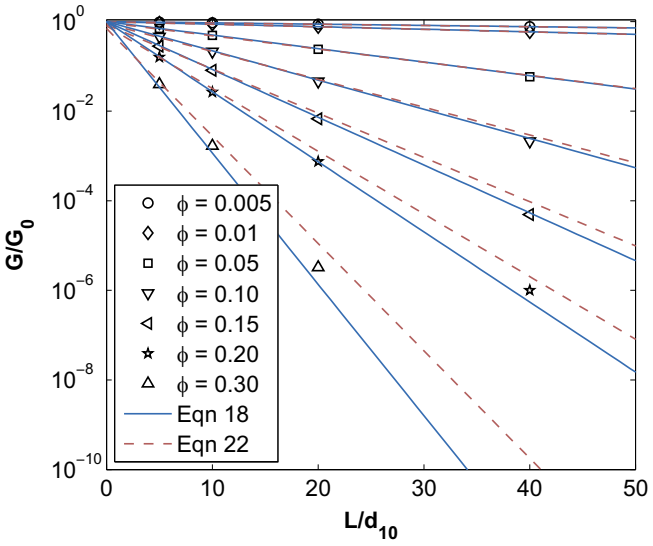

Fig. 5. Photon extinction as a function of system depth L in case of normal *PSD*.

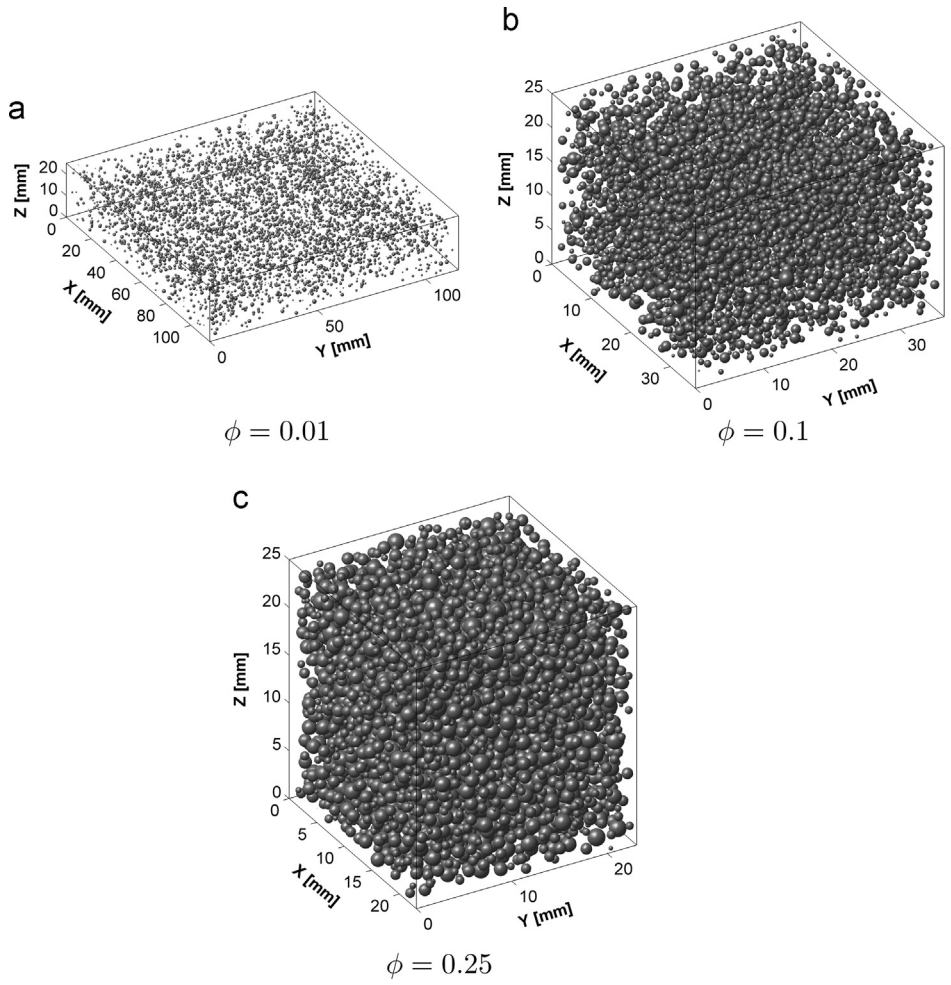

Fig. 4. Virtual box ($L = 25$) with normally distributed particles placed within, $d_{10} = 1$, at different particle volume fraction. (a) $\phi = 0.01$. (b) $\phi = 0.1$. (c) $\phi = 0.25$.

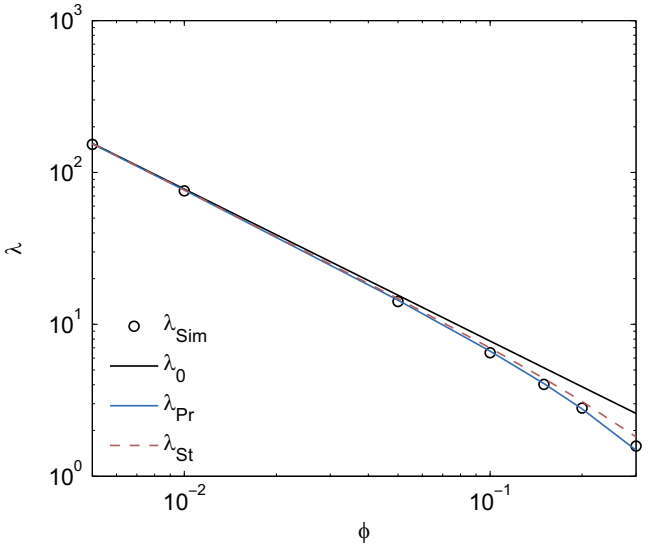

Fig. 6. Extinction length λ as a function of particle concentration in case of normal particle size distribution ($d_{10}=1$, $d_{32}=1.164$).

Notably, the reported simulated data confirm that light extinction closely follows a *Lambert–Beer* law, with exponential extinction coefficient depending on particle concentration. This is in agreement with both Eqs. (18) and (22), whose predictions are also reported in Fig. 5 as red dashed lines and blue solid lines respectively.

One of the main differences between Eqs. (18) and (22) can be immediately noted from Fig. 5: in fact, Eq. (22) predicts G/G_0 values smaller than unity at $L=0$, while Eq. (18), closer in its form to the original Lambert–Beer law, gives $G/G_0=1$ at $L=0$. This difference comes out because in stereology calculations, particles are allowed to be cut by the planes limiting the observed volume (*i.e.* the planes at $z=0$ and $z=L$). Hence, in a hypothetical zero-thickness slab, particles cross-section will be present, giving rise to the relevant light obscuration and G/G_0 values smaller than unity. However, in photo-reactors applications, this is not allowed, and Eq. (22) can be considered for comparison purposes only at L values larger than average particle diameter. Nevertheless, stereological model predictions show a fairly good agreement with simulated data.

The predictions obtained by the statistical model here proposed are also reported in Fig. 5. In all cases investigated, an $\chi_{av}=0.95$ value was used, obtaining excellent data agreement at all particle concentrations analyzed. This value, found by fitting the simulated data on extinction length, was also found to remain the same when different PSD are considered, see Fig. 7. Moreover, its value is in line with physical expectations, as discussed earlier.

In order to better grasp how the main physical parameters affect the radiation field, in Fig. 6 the dependence of the extinction length (as computed by the different models presented here) on particle concentration is shown. On the same figure, the simulated data on the extinction length are reported (λ_{sim}). These values were obtained by simple linear regression of the simulated ln (G/G_0) *vs* L data reported for instance in Fig. 5.

The analysis of the λ_{sim} values highlights that:

- Exact match is found between λ_{sim} and λ_0 in case of diluted suspensions ($\phi\to 0$), confirming that the extension of previous models (Brucato and Rizzuti, 1997a) to the case of polydispersed particles is substantially correct. This observation also gives a further indirect validation of the proposed probabilistic approach. In fact, the equation proposed by Brucato and Rizzuti (1997a) for prediction of λ_0 value in case of single-sized particles was experimentally validated. The extension of that model equation to polydispersed PSD is therefore validated. Moreover, the substantial correctness of some of the assumptions at the basis of the present model is confirmed, such as those regarding the photon absorption and scattering by the fluid, the validity of geometric optics, absence of emission by the heterogeneous system.
- As particle concentration is increased, smaller values of the extinction length are found with respect to the value computed by means of the diluted model (λ_0).

Both proposed equations for estimating the extinction length (Eqs. (18) and (22)) are taken into account and compared with simulation data: as it can be seen, both model are able to catch the main trend, but the probabilistic approach here proposed results in a quite closer agreement (deviation from pseudo-experimental data is within $-0.99/+1.8\%$ for the probabilistic approach here proposed and within $-0.0/+8.7\%$ for the stereological approach for normal particle size distribution).

Similar comments apply to the other simulations ran with different particle size distributions, whose results are shown in Fig. 7. Data are reported in terms of pseudo-experimental (λ_{sim}) or calculated (λ_{Pr}, λ_{St}) values, normalized by the relevant value computed by means of the dilute model λ_0, in order to enhance the differences between the models. The different ability of the probabilistic (λ_{Pr}, blue solid lines) and the stereological (λ_{St}, red dashed lines) models to reproduce the pseudo-experimental extinction length data becomes apparent in this figure. As it can be seen, only the probabilistic model is able to correctly simulate the Monte Carlo generated pseudo-experimental data obtained.

The comparison of model predictions and simulated data gives also a strong indication about the range of applicability of the model for dilute systems (Eq. (8)). Such model gives rise to an overestimation of the extinction length of less than 2.9% at $\phi=0.01$, while the maximum discrepancy decrease to 1.9% at $\phi=0.005$. One can therefore affirm that an error smaller than 2% is surely obtained from Eq. (8), provided that the particles concentration do not exceed $\phi=0.005$. Notably, it is possible to relate such values to the level of particles steric hinderance by using the concept of mean separation between particles $\bar{s}$. This value can be computed by a simple equation (Underwood, 1970):

$$\bar{s}=4\frac{1-\phi}{S_v} \tag{30}$$

For spherical particles, the mean separation between particles is a simple function of volume fraction and average particle diameter d_{32}:

$$\bar{s}=\frac{2}{3}\frac{1-\phi}{\phi} \tag{31}$$

At $\phi=0.005$, the mean separation between particles is about $133d_{32}$. A convenient limit to consider the suspension as dilute (in which steric hindrance effects are negligible) could be estimated by imposing a mean particle separation of at least $150d_{32}$.

Notably, the good agreement observed between the probabilistic model, and the pseudo-experimental λ_{sim} values clearly further confirms that the extinction length actually depends on particle d_{32}. In all cases investigated, an equally good agreement is obtained when the d_{32} value is adopted to account for particles polidispersity: the adoption of any other average size would have resulted into discrepancies with respect to the pseudo-experimental data, at least for the cases here investigated. It is however worth reminding that quite different PSD shapes were adopted here, giving rise to a harsh test for the proposed model, so confirming the effectiveness of the proposed model.

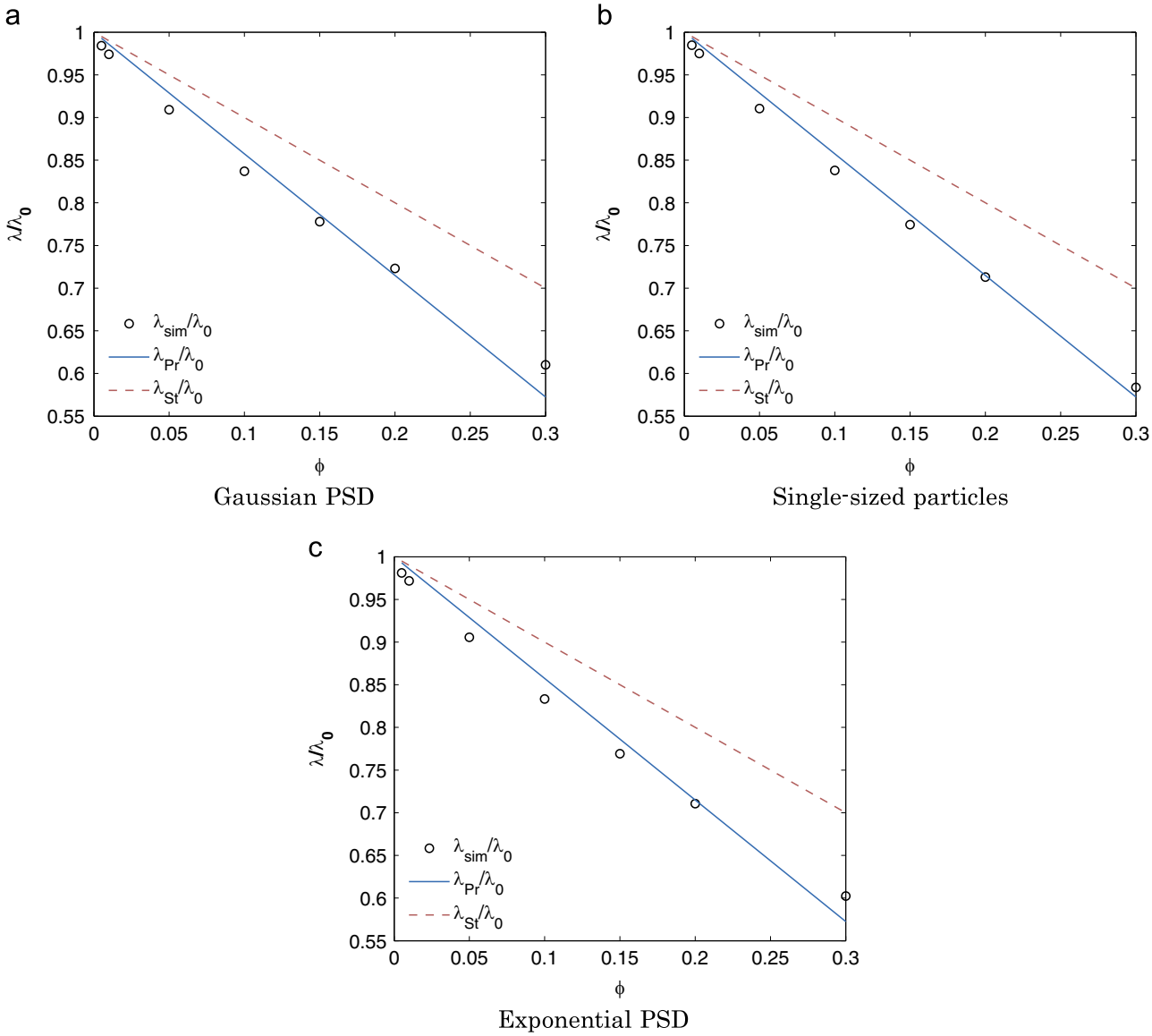

Fig. 7. Dimensionless extinction length values obtained by simulations and relevant predictions for different particle size distributions. (a) Gaussian PSD. (b) Single-sized particles. (c) Exponential PSD.

6. Model extension to absorbing/scattering particles

The results so far obtained show that under the aforementioned hypotheses, that include the assumption that all photon/particle interactions invariably result into photon absorption, it is possible to estimate the light extinction length through simple equations, even for dense systems showing a particle size distribution. It is worth mentioning here that, also for these systems, the above quoted assumption may be removed still retaining the simple closed form solution. This can be done, for instance, by extending the previously developed six-flux model (SFM) for dilute single-sized particle dispersions (Brucato et al., 2006) to the present case. The above hypothesis is therefore substituted by the following set of hypothesis:

- a photon hitting a particle is allowed to be scattered or absorbed, with a scattering probability (albedo) given by R;
- with respect to the incident radiation, scattering may only occur only along the six directions of a Cartesian 3-dimensional system of coordinates; the relevant scattering probabilities are p_f p_b and p_s in the forward, backward and side-ward directions respectively;

In this section the analytical solution previously obtained by Brucato et al. (2006) is adapted to present paper results on the probability of photon/particle interaction in dense size-distributed systems. Notably, the SFM was shown to be quite accurate in predicting photo-reactor radiant field features. The following closed form equations are obtained for the forward (G), backward (g_b) sideway (g_s) radiant fluxes:

$$\frac{G}{G_0}=\frac{1}{1-\gamma}\exp\left(-\frac{x}{\lambda_{corr}}\right)\left[1-\gamma\exp\left(-\frac{2x}{\lambda_{corr}}\right)\right] \tag{32}$$

$$\frac{g_b}{G_0}=\frac{1-\sqrt{1-R_{corr}^2}}{R_{corr}(1-\lambda)}\exp\left(-\frac{x}{\lambda_{corr}}\right)-\gamma\frac{1+\sqrt{1-R_{corr}^2}}{R_{corr}(1-\lambda)}\exp\left(\frac{x}{\lambda_{corr}}\right) \tag{33}$$

$$g_s=\frac{Rp_s}{1-R\left(p_f+p_b-2p_s\right)}(G+g_b) \tag{34}$$

where γ and R_{corr} are two dimensionless parameters defined for the SFM on the basis of system physical parameters, and λ_{corr} is the extinction length in the system under investigation.

$$R_{corr}=b/a \tag{35}$$

$$a = 1 - Rp_f - \frac{4R^2 p_s^2}{1 - R\left(p_f + p_b + 2p_s\right)} \tag{36}$$

$$b = Rp_b + \frac{4R^2 p_s^2}{1 - R\left(p_f + p_b + 2p_s\right)} \tag{37}$$

$$\gamma = \frac{1 - \sqrt{1 - R_{corr}^2}}{1 + \sqrt{1 - R_{corr}^2}} \exp\left(-\frac{2L}{\lambda_{corr}}\right) \tag{38}$$

$$\lambda_{corr} = \frac{\lambda_{Pr}}{a\sqrt{1 - R_{corr}^2}} \tag{39}$$

It is also possible to compute the transmitted (G_L) and reflected ($g_{b,0}$) radiative fluxes as follows:

$$\frac{G_L}{G_0} = \frac{1}{1-\gamma}\left(\frac{2\sqrt{1 - R_{corr}^2}}{1 + \sqrt{1 - R_{corr}^2}}\right) \exp\left(-\frac{L}{\lambda_{corr}}\right) \tag{40}$$

$$\frac{g_{b,0}}{G_0} = \frac{1}{R_{corr}}\left(1 - \frac{1+\gamma}{1-\gamma}\sqrt{1 - R_{corr}^2}\right) \tag{41}$$

Finally, the Local Volumetric Rate of Photon Absorption (*LVRPA*), that is necessary for the analysis and design of photocatalytic reactors, can be also calculated on the basis of equations developed for the SFM:

$$\frac{LVRPA}{G_0} = \frac{\left(R_{corr} - 1 + \sqrt{1 - R_{corr}^2}\right) e^{-x/\lambda_{corr}}}{R\lambda_{corr}(1-\gamma)} - \frac{\left(R_{corr} - 1 - \sqrt{1 - R_{corr}^2}\right) e^{x/\lambda_{corr}}}{R\lambda_{corr}(1-\gamma)} \tag{42}$$

The average value of *LVRPA* within the reactor volume can be computed as:

$$\overline{LVRPA} = \frac{G_0 - G_L - g_{b,0}}{L} \tag{43}$$

As the SFM had already been validated for dilute systems by means of Monte Carlo simulations, (Brucato et al., 2006), while the dense size-dispersed model has been validated here, the above set of equations may be regarded as being validated as well to treat radiant field features in case of well mixed particle suspensions, provided that model assumptions about particles and fluid properties hold true.

7. Conclusions

A very simple model was set-up for the prediction of radiant field in heterogeneous systems. In this model, a suspension of *black* particles in a perfectly transparent continuous phase is considered. Particles are large enough to make classical optics assumptions valid.

For these cases, the proposed model allows accurate estimation of light extinction, being known the average particle concentration and size.

The model was validated by means of Monte Carlo simulations, as well as compared with literature correlations, showing a quite good agreement with simulated data.

The main feature of the proposed model is its simplicity, that allows one to get immediate grasp on the effect of physical, assessable parameters on radiant field, even in the complex case of concentrated suspensions.

Notation

A'	fractional image area occupied (−)
A	reactor cross sectional area (m^2)
$a_{p,i}$	area projected by i-th particle (m^2)
d_{32}	Sauter mean diameter $\sum d_p^3 / \sum d_p^2$ (m)
d_{10}	Arithmetic mean diameter (m)
d_p	particle characteristic length (m)
G	forward radiant flux (*einstein* $s^{-1}m^{-2}$)
G_0	radiant flux at the reactor wall $L = 0$ (*einstein* $s^{-1}m^{-2}$)
g_b	backward radiant flux (*einstein* $s^{-1}m^{-2}$)
g_s	side − way radiant flux (*einstein* $s^{-1}m^{-2}$)
L	optical path, reactor thickness (m)
N_p	number of particle within reactor (#)
$p_{f,b,s}$	probabilities (#)
R	albedo (intrinsic particle reflectance) (#)
S_v	specific interfacial area (m^{-1})
$\overline{s}$	average particle separation (m)
x	length of the reactor (m)
α	Particle volume$/d_p^3$ (−)
β	particle projected area$/d_p^2$ (−)
λ_{sim}	simulated extinction length (m)
λ_0	extinction length (diluted case) (m)
λ_{Pr}	extinction length (prob. approach) (m)
λ_{St}	extinction length (stereological) (m)
ϕ	particle volume fraction (−)
ψ	fractional area not sterically inhibited by other particles position (−)
χ	particle fractional area inhibiting other particles position (−)

Acknowledgments

This work was financially supported through the project "BIO4BIO - Biomolecular and Energy valorization of residual biomass from Agroindustry and Fishing Industry" led by the Cluster Sicily Agrobio and Fishing Industry and funded by the Italian Research Fund (PON R & C 2007–2013, DD 713/Ric. - PON02 00451 3362376.

References

Brandi, R., Alfano, O., Cassano, A.E., 1996. Modeling of radiation absorption in a flat plate photocatalytic reactor. Chem. Eng. Sci. 51, 3169.

Brandi, R., Alfano, O., Cassano, A.E., 1999. Rigorous model and experimental verification of the radiation field in a flat plate solar collector simulator employed for photocatalytic reactions. Chem. Eng. Sci. 54, 2817–2827.

Brandi, R., Alfano, O., Cassano, A.E., 2000. Evaluation of radiation absorption in slurry photocatalytic reactors. part i: assessment of methods in use and new proposal. Environ. Sci. Technol. 34, 2623–2630.

Brucato, A., Cassano, A., Grisafi, F., Montante, G., Rizzuti, L., Vella, G., 2006. Estimating radiant fields in flat heterogeneous photoreactors by the six-flux model. AIChE J. 52 (11), 3882–3890.

Brucato, A., Rizzuti, L., 1997a. Simplified modeling of radiant fields in heterogeneous photoreactors. 1. case of zero reflectance. Ind. Eng. Chem. Res. 36, 4740–4747.

Brucato, A., Rizzuti, L., 1997b. Simplified modeling of radiant fields in heterogeneous photoreactors. 2. limiting "two-flux" model for the case of reflectance greater than zero. Ind. Eng. Chem. Res. 36, 4748–4755.

Brucato, A., Rizzuti, L., Esterkin, C., Alfano, O., Cassano, A., 1997. Una aproximacion probabilistica al modelado de la maxima absorcion de radiacion en reactores fotocataliticos. In: Anales AFA, volumen 9. 82 reunion de la Asocicion Fisica Argentina, San Luis, pp. 137–140.

Busciglio, A., Grisafi, F., Scargiali, F., Brucato, A., 2010. On the measurement of local gas hold-up and interfacial area in gas-liquid contactors via light sheet and image analysis. Chem. Eng. Sci. 65 (12), 3699–3708.

Cassano, A., Alfano, O., 2000. Reaction engineering of suspended solid heterogeneous photocatalytic reactors. Catal. Today 58, 167–197.

Cassano, A., Martin, C., Brandi, R., Alfano, O., 1995. Photoreactor analysis and design: fundamentals and applications. Ind. Eng. Chem. Res. 34, 2155.

Davydov, L., Smirniotis, P.G., Pratsinis, S.E., 1999. Novel differential reactor for the measurement of overall quantum yields. Ind. Eng. Chem. Res. 38, 1376–1383.

Hammersley, J., Handscomb, D. (Eds.), 1983. Monte Carlo Methods. Chapman and Hall Ltd., London.

Heinrich, J., Niizawa, I., Botta, F., Trombert, A., Irazoqui, H., 2012. Analysis and design of photobioreactors for microalgae production ii: experimental validation of a radiation field simulator based on a monte carlo algorithm. Photochem. Photobiol. 88, 952–960.

Heinrich, J., Niizawa, I., Botta, F., Trombert, A., Irazoqui, H., 2013. Stratification of the radiation field inside a photobioreactor during microalgae growth. Photochem. Photobiol. 89, 1127–1134.

Katsuda, T., Arimoto, T., Igarashi, K., Azuma, M., Kato, J., Takakuwa, S., Ooshima, H., 2000. Light intensity distribution in the externally illuminated cylindrical photo-bioreactor and its application to hydrogen production by rhodobacter capsulatus. Biochem. Eng. J. 5, 157–164.

Li, J., Xu, N., Su, W., 2003. Online estimation of stirred-tank microalgal photobioreactor cultures based on dissolved oxygen measurement. Biochem. Eng. J. 14, 51–65.

Li Puma, G., Brucato, A., 2007. Dimensionless analysis of slurry photocatalytic reactors using two-flux and six-flux radiation absorption-scattering models. Catal. Today 122, 78–90.

Li Puma, G., Khor, J., Brucato, A., 2004. Modelling of an annular photocatalytic reactor for water purification: oxidation of pesticides. Environ. Sci. Technol. 38, 3737–3745.

Molina Grima, E., Acien Fernandez, F., Garcia Camacho, F., Chisti, Y., 1999. Photobioreactors: light regime, mass transfer, and scaleup. J. Biotechnol. 70, 231–247.

Motegh, M., van Ommen, J., Appel, P., Mudde, R., Kreutzer, M., 2013. Bubbles scatter light, yet that does not hurt the performance of bubbly slurry photocatalytic reactors. Chem. Eng. Sci. 100, 506–514.

Otalvaro-Marin, H., Mueses, M., Machuca-Martinez, F., 2014. Boundary layer of photon absorption applied to heterogeneous photocatalytic solar flat plate reactor design. Int. J. Photoenergy 2014, 930439.

Overby, D., Johnson, M., 2005. Studies on depth of field effects in microscopy supported by numerical simulations. J. Microsc. 220 (3), 176–189.

Palma, V., Sannino, D., Vaiano, V., Ciambelli, P., 2010. Fluidized-bed reactor for the intensification of gas-phase photocatalytic oxidative dehydrogenation of cyclohexane. Ind. Eng. Chem. Res. 49, 10279–10286.

Pasquali, M., Santarelli, F., Porter, J., Yue, P., 1996. Radiative transfer in photocatalytic systems. AIChE J. 42, 532.

Romero, R., Alfano, O., Cassano, A., 1997. Cylindrical photocatalytic reactors. radiation absorption and scattering effects produced by suspended fine particles in an annular space. Ind. Eng. Chem. Res. 36, 3094–3109.

Santarelli, F., 1985. Photoelectrochemistry, photocatalysis and photoreactors. Fundamentals and developments. Reidel, Dordrecht, Ch. Radiative transfer in photochemical processes, p. 549.

Spadoni, G., Bandini, E., Santarelli, F., 1978. Scattering effects in photosentized reactions. Chem. Eng. Sci. 33, 517.

Su, W., Li, J., Xu, N., 2003. State and parameter estimation of microalgal photobioreactor cultures based on local irradiance measurement. J. Biotechnol. 105, 165–178.

Underwood, E., 1970. Quantitative Stereology. Addison-Wesley, Reading, MA.

Yun, Y.-S., Park, J., 2001. Attenuation of monochromatic and polychromatic lights in chlorella vulgaris suspensions. Appl. Microbiol. Biotechnol. 55, 765–770.